Nanoscale

COMMUNICATION

View Article Online
View Journal | View Issue

Unadulterated BODIPY-dimer nanoparticles with high stability and good biocompatibility for cellular imaging†

Cite this: *Nanoscale*, 2014, **6**, 5662

Received 26th January 2014
Accepted 25th March 2014

DOI: 10.1039/c4nr00521j

www.rsc.org/nanoscale

Zhensheng Li,[a] Min Zheng,[b] Xingang Guan,[ac] Zhigang Xie,*[a] Yubin Huang[a] and Xiabin Jing[a]

Purely organic nanoparticles based on a BODIPY dimer, **BDY-NPs**, have been prepared for the first time using a nanoprecipitation procedure. The fluorescent nanoparticles have high physical homogeneity, good stability in water, and low cytotoxicity, which are suitable for cell imaging.

Fluorescent nanoparticles (NPs) have been demonstrated to be ideal probes for a wide range of applications such as chemical sensing, live cell imaging and theranostics[1–5] because of their high brightness and improved photostability. For example, inorganic semiconductor quantum dots (QDs) are highly emissive and photostable and can be used as cell labeling reagents, however, the toxicity caused by heavy metal ions is a critical barrier for their biomedical applications.[6–11] On the other hand, fluorescent carbon dots have been developed because of their better biocompatibility and lower cytotoxicity,[12–14] nevertheless, rare yellow- and red-emitting carbon dots are explored, which severely limits broad applications of carbon dots in the bio-imaging field due to the low organ penetration depth of blue or green light. Hence, new fluorescent nanoparticles with intense long-wavelength emission, excellent photostability, high biocompatibility and low cytotoxicity are highly desired to satisfy multiplexed biological detection and imaging.

BODIPY (4-difluoro-4-bora-3*a*,4*a*-diaza-*s*-indacene) dyes have received considerable interest due to their promising applications as imaging agents because of their many outstanding and desirable properties such as high absorption coefficients, sharp emissions, high fluorescence quantum yields, and excellent chemical and photostability.[15–18] In spite of this, it is regrettable that most BODIPY dyes are not soluble in water-based biological media, which hinders their biomedical applications. One appealing way to overcome this problem is preparation of highly stable BODIPY nanoparticles in aqueous solution. Fluorescent BODIPY nanoparticles are usually made by physically entrapping dyes in the polymeric bulk, or by covalently attaching the dyes to the nanoparticles.[19–21] However, one of the main problems of the former approach is that the fluorophores can leak out of the particles with time,[22] and the latter is very complicated and time-consuming.[23]

Recently, Tang *et al.* have developed several organic dots based on aggregation-induced emission (AIE) for cell tracing or vasculature imaging.[24–28] Although these particles exhibited unique optical properties, they required organic solvents as cosolvents or lipid–PEG derivatives as the encapsulation matrix. To the best of our knowledge, few fluorescent nanoparticles synthesized from organic dyes without any cosolvent or encapsulation were ever explored.[24]

Herein we report a facile, convenient and versatile approach to prepare highly water-soluble, red emissive BODIPY nanoparticles (**BDY-NPs**). These nanoparticles can function as intrinsic red fluorophores for bioimaging with good biocompatibility and high stability in water. The feasible synthesis method and outstanding properties of **BDY-NPs** provide a novel approach for exploring a new generation of organic fluorescent probes.

The synthesis routes and spectroscopic properties of three novel BODIPY derivatives (**BDY 1**, **BDY 2**, and **BDY 3**) bearing tetraphenylethene (TPE) groups have been reported (Fig. 1).[29] The bulky TPE groups attached laterally to the rigid core suppress the intermolecular π–π interaction and lead to intense fluorescence of BODIPY in organic solution and the solid state. However, these dyes are not water-soluble. In the course of study on the AIE phenomenon of these BODIPYs, we observed that the fluorescent particles formed from **BDY 1** in water after evaporating tetrahydrofuran (THF) completely. The synthesis

[a]*State Key Laboratory of Polymer Physics and Chemistry, Changchun Institute of Applied Chemistry, Chinese Academy of Sciences, 5625 Renmin Street, Changchun 130022, P. R. China. E-mail: xiez@ciac.ac.cn; Tel: +86-431-85262779*

[b]*State Key Laboratory of Luminescence and Applications, Changchun Institute of Optics, Fine Mechanics and Physics, CAS, 3888 East Nanhu Rd. Changchun, Jilin, 130033, P. R. China*

[c]*Life Science Research Center, Beihua University, Jilin, 132013, P. R. China*

† Electronic supplementary information (ESI) available. See DOI: 10.1039/c4nr00521j

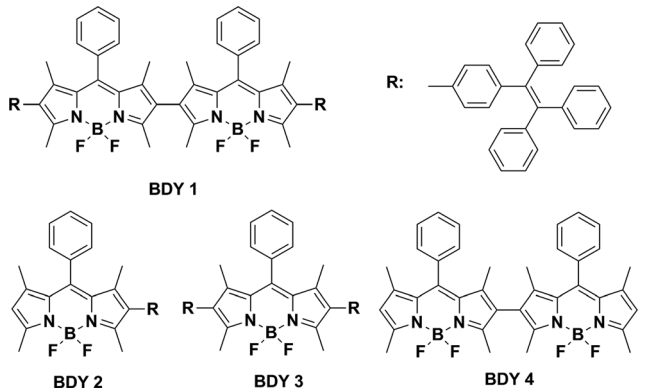

Fig. 1 Structures of BODIPY dyes.

procedure of BODIPY nanoparticles is shown below: briefly, 5 mL of **BDY 1** (0.05 mg mL^{-1}) solution in THF was added into 5 mL of water at room temperature with vigorous stirring overnight, and finally a red, transparent and fluorescent nanoparticle suspension was formed after evaporation of THF.

The morphology and structure of **BDY-NPs** were confirmed by scanning electron microscopy (SEM) and transmission electron microscopy (TEM). Fig. 2a shows the SEM image of the **BDY-NPs**, which were cast from the water solution onto a Si wafer. It clearly shows the isolated spherical particles with an average diameter of (104.0 ± 12.2) nm. While the TEM image (Fig. 2b) indicates that the size of the as-prepared **BDY-NPs** is distributed in the range from 90.0 to 123.0 nm, with an average size of 106.7 nm, which is consistent with the result of SEM. Well-resolved lattice fringes are observed from high-resolution TEM images corresponding to *d* spacing values of 0.28 and 0.33 nm (Fig. 2c–e), which are close to the (020) and (002) planes of graphitic carbon, respectively,[30] indicating the graphitic nature of **BDY-NPs**. These primary nanoparticles form aggregates in the 106.7 ± 16.1 nm size range.

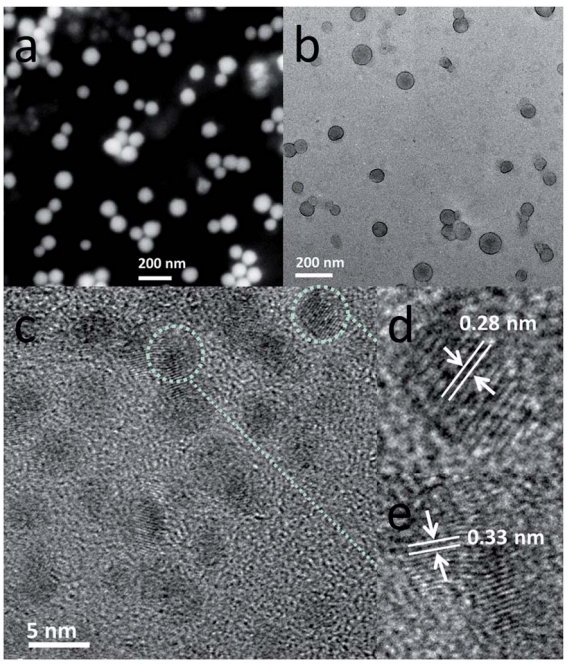

Fig. 2 (a) SEM, (b) TEM and (c) HRTEM images of **BDY-NPs**. (d and e) Typical single **BDY-NPs** with lattice parameters of 0.28 nm and 0.33 nm, respectively.

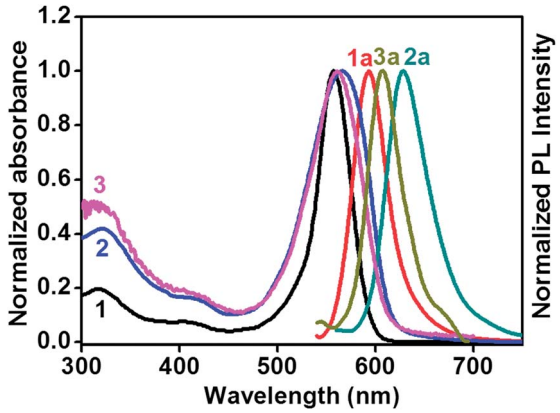

Fig. 3 UV-vis absorption and photoluminescence spectra of **BDY 1** in THF (1 and 1a), in the solid state (2 and 2a) and **BDY-NPs** in water (3 and 3a), respectively.

Fig. 3 shows the UV-vis absorption and photoluminescence spectra of **BDY-NPs** in water and **BDY 1** in THF solution or the solid state. They exhibit similar spectroscopic spectra, but the maximum absorption and emission-wavelengths are slightly different. That is, the absorption and emission bands of **BDY-NPs** peaked at 562 nm and 609 nm respectively, which are larger than those in THF solution and smaller than those in the solid state, indicating that the fluorogens aggregate into a particle form. The quantum yield (Φ) is measured to be 5.0% by using rhodamine 6G as the reference, which is lower than that in THF (Φ_{THF} = 53.0%), but close to that in the powdery form (Φ_{solid} = 4.0%).[29] The photostability of **BDY-NPs** was also investigated by spectroscopic measurements. After UV light irradiation, the absorption and emission spectra of **BDY-NPs** change little (Fig. S1, ESI†), while **BDY 1** in THF was photodegraded in 10 minutes, indicating the significantly improved photostability of **BDY-NPs**.

To explore the mechanisms of the formation of **BDY-NPs**, a number of BODIPY analogues (Fig. 1) were synthesized. No nanoparticles, only precipitates, were obtained when **BDY 2** and **BDY 3** were used as starting materials. These results indicate that the bulky TPE groups do not play a crucial part in the formation of nanoparticles. Therefore, we deduce that the dimer structure of **BDY 1** may be the key factor. In order to confirm our hypothesis, another BODIPY dimer without TPE groups (**BDY 4**) was used to synthesize nanoparticles with a similar self-organizing precipitation method. The result was in accordance with our anticipation that nanoparticles (**BDY 4 NPs**) were obtained successfully with a size of about 250 nm determined by DLS (Fig. S2†), which is larger than that of **BDY-NPs** perhaps because **BDY 4** without TPE modification aggregated more easily. However, **BDY 4 NPs** do not show fluorescence. Furthermore, **BDY 4 NPs** are not stable in water, and they aggregate into larger particles that precipitate out of the solution after 1 day. In contrast, **BDY-NPs** are much more stable, the suspension solution is very clear even after two months

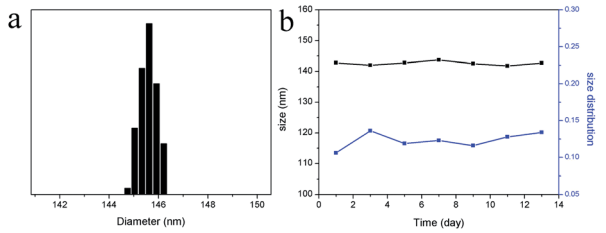

Fig. 4 Size and size distribution of BDY-NPs in water (a) and their changes with different times (b) determined by DLS.

(Fig. S3†). The diameter of **BDY-NPs** determined by dynamic light scattering (DLS) was 142 nm (Fig. 4a), slightly bigger than that observed by TEM. The size and size distribution do not show any changes even in two weeks (Fig. 4b). We believe that the two bulky TPE groups of **BDY 1** prevent further agglomeration of **BDY-NPs** and help them to maintain high stability in water.

The biocompatibility of nanomaterials is very important for their biomedical applications.[31–33] Besides surface modification and composition, the size (<100 nm) and shape of nanoparticles also matter in cellular uptake and behaviors.[34,35] In this work, the biocompatibility of **BDY-NPs** was evaluated using HeLa cells. Fig. S4† shows the morphology of HeLa cells when they have been incubated with different concentrations of **BDY-NPs** for 24 h. It can be seen that all the cells maintain their normal morphology. As shown in Fig. S4d,† no obvious cytotoxicity was observed even at a concentration of 40 μg mL^{-1} for **BDY-NPs** after 24 h, which indicates that **BDY-NPs** are biocompatible with living cells. In contrast, **BDY 1** indicates seriously deleterious effects on the cell metabolism (Fig. S5†). The comparison further demonstrated the excellent biocompatibility of the fluorescent nanoparticles, which facilitated us to explore the possibility of cellular imaging.

To study the potential biomedical applications of **BDY-NPs**, cellular imaging was examined using confocal laser scanning microscopy (CLSM). As shown in Fig. 5, bright red fluorescence is observed when cells are incubated with 5 μg mL^{-1} of **BDY-NPs** for 2 h. From CLSM images, it can be seen that **BDY-NPs** mainly locate at the cytoplasm, which differs from the blue cell nuclei dyed with 4′,6-diamidino-2-phenylindole (DAPI). These results show the **BDY-NPs** could be uptaken by HeLa cells and located at the cytoplasm. Due to no surface modification or introduction of organelle-targeting groups, such as a triphenylphosphonium cation and morpholine,[36,37] the **BDY-NPs** do not show specific targeting. However, the low concentration for cellular imaging, together with good water-solubility, suggested their potential for biological imaging applications.

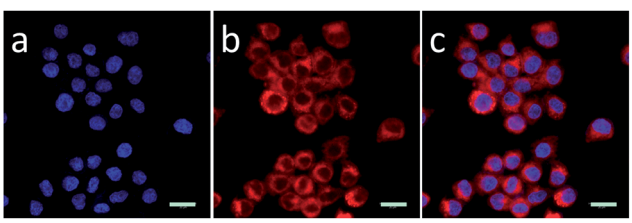

Fig. 5 CLSM images of HeLa cells incubated with BDY-NPs at the concentration of 5 μg mL^{-1} for 1 h. (a) DAPI-stained nuclei image, (b) BDY-NP image, and (c) merged image; the scale bar of the images is 20 μm.

In summary, fluorescent BODIPY nanoparticles were prepared by a precipitation method using a pure BODIPY dimer. Due to the bulky TPE groups and the dimer structure, **BDY-NPs** with a diameter of 107 nm are highly stable in water at room temperature. The fluorescent nanoparticles show good photostability and biocompatibility compared with **BDY 1** in solution. These incredible features make the unadulterated organic nanoparticles promising for developing novel fluorescent probes for bioimaging applications.

Acknowledgements

The project was supported by the National Natural Science Foundation of China (Project no. 91227118 and 21201159).

Notes and references

1 D. Liu, R. C. Huxford and W. Lin, *Angew. Chem., Int. Ed.*, 2011, **50**, 3696–3700.
2 Z. Yang, J. H. Lee, H. M. Jeon, J. H. Han, N. Park, Y. He, H. Lee, K. S. Hong, C. Kang and J. S. Kim, *J. Am. Chem. Soc.*, 2013, **135**, 11657–11662.
3 Z. Zhang, J. Wang and C. Chen, *Adv. Mater.*, 2013, **25**, 3869–3880.
4 K. M. L. Taylor-Pashow, J. Della Rocca, Z. Xie, S. Tran and W. Lin, *J. Am. Chem. Soc.*, 2009, **131**, 14261–14263.
5 Z. Xie, L. Ma, K. E. deKrafft, A. Jin and W. Lin, *J. Am. Chem. Soc.*, 2010, **132**, 922–923.
6 D. Deng, L. Qu, S. Achilefu and Y. Gu, *Chem. Commun.*, 2013, **49**, 9494–9496.
7 M.-E. Lecavalier, M. Goulet, C. N. Allen, L. Beaulieu and D. Lariviere, *Chem. Commun.*, 2013, **49**, 11629–11631.
8 Y. Nakane, Y. Tsukasaki, T. Sakata, H. Yasuda and T. Jin, *Chem. Commun.*, 2013, **49**, 7584–7586.
9 Z. Qu, X. Zhou, L. Gu, R. Lan, D. Sun, D. Yu and G. Shi, *Chem. Commun.*, 2013, **49**, 9830–9832.
10 F. Erogbogbo, C.-W. Chang, J. L. May, L. Liu, R. Kumar, W.-C. Law, H. Ding, K. T. Yong, I. Roy, M. Sheshadri, M. T. Swihart and P. N. Prasad, *Nanoscale*, 2012, **4**, 5483–5489.
11 D. Qu, M. Zheng, P. Du, Y. Zhou, L. Zhang, D. Li, H. Tan, Z. Zhao, Z. Xie and Z. Sun, *Nanoscale*, 2013, **5**, 12272–12277.
12 M. Zheng, Z. Xie, D. Qu, D. Li, P. Du, X. Jing and Z. Sun, *ACS Appl. Mater. Interfaces*, 2013, **5**, 13242–13247.
13 B. Chen, F. Li, S. Li, W. Weng, H. Guo, T. Guo, X. Zhang, Y. Chen, T. Huang, X. Hong, S. You, Y. Lin, K. Zeng and S. Chen, *Nanoscale*, 2013, **5**, 1967–1971.
14 S. Chandra, P. Das, S. Bag, D. Laha and P. Pramanik, *Nanoscale*, 2011, **3**, 1533–1540.
15 W. Li, L. Li, H. Xiao, R. Qi, Y. Huang, Z. Xie, X. Jing and H. Zhang, *RSC Adv.*, 2013, **3**, 13417–13421.
16 W. Li, Z. Xie and X. Jing, *Catal. Commun.*, 2011, **16**, 94–97.

17 S. K. Yang, X. Shi, S. Park, T. Ha and S. C. Zimmerman, *Nat. Chem.*, 2013, **5**, 692–697.
18 C. Zhang, J. Zhao, S. Wu, Z. Wang, W. Wu, J. Ma, S. Guo and L. Huang, *J. Am. Chem. Soc.*, 2013, **135**, 10566–10578.
19 F. E. Alemdaroglu, S. C. Alexander, D. Ji, D. K. Prusty, M. Böersch and A. Herrmann, *Macromolecules*, 2009, **42**, 6529–6536.
20 C. Grazon, J. Rieger, R. Meallet-Renault, B. Charleux and G. Clavier, *Macromolecules*, 2013, **46**, 5167–5176.
21 R. Sauer, A. Turshatov, S. Baluschev and K. Landfester, *Macromolecules*, 2012, **45**, 3787–3796.
22 Y. Jin, F. Ye, M. Zeigler, C. Wu and D. T. Chiu, *ACS Nano*, 2011, **5**, 1468–1475.
23 S. Zhu, J. Zhang, J. Janjanam, J. Bi, G. Vegesna, A. Tiwari, F.-T. Luo, J. Wei and H. Liu, *Anal. Chim. Acta*, 2013, **758**, 138–144.
24 Y. Yu, C. Feng, Y. Hong, J. Liu, S. Chen, K. M. Ng, K. Q. Luo and B. Z. Tang, *Adv. Mater.*, 2011, **23**, 3298–3302.
25 K. Li, D. Ding, Q. Zhao, J. Sun, B. Z. Tang and B. Liu, *Sci. China: Chem.*, 2013, **56**, 1228–1233.
26 K. Li, Z. Zhu, P. Cai, R. Liu, N. Tomczak, D. Ding, J. Liu, W. Qin, Z. Zhao, Y. Hu, X. Chen, B. Z. Tang and B. Liu, *Chem. Mater.*, 2013, **25**, 4181–4187.
27 D. Ding, C. C. Goh, G. Feng, Z. Zhao, J. Liu, R. Liu, N. Tomczak, J. Geng, B. Z. Tang, L. G. Ng and B. Liu, *Adv. Mater.*, 2013, **25**, 6083–6088.
28 K. Li, W. Qin, D. Ding, N. Tomczak, J. Geng, R. Liu, J. Liu, X. Zhang, H. Liu, B. Liu and B. Z. Tang, *Sci. Rep.*, 2013, **3**, 1150.
29 Z. Li, Y. Chen, X. Lv and W.-F. Fu, *New J. Chem.*, 2013, **37**, 3755–3761.
30 J. Tang, B. Kong, H. Wu, M. Xu, Y. Wang, Y. Wang, D. Zhao and G. Zheng, *Adv. Mater.*, 2013, **25**, 6569–6574.
31 X. Zhang, S. Wang, L. Xu, L. Feng, Y. Ji, L. Tao, S. Li and Y. Wei, *Nanoscale*, 2012, **4**, 5581–5584.
32 X. Zhang, X. Zhang, S. Wang, M. Liu, L. Tao and Y. Wei, *Nanoscale*, 2013, **5**, 147–150.
33 C. Y. Zhu, B. Yang, Y. A. Zhao, C. K. Fu, L. Tao and Y. Wei, *Polym. Chem.*, 2013, **4**, 5395–5400.
34 Y.-L. Wu, N. Putcha, K. W. Ng, D. T. Leong, C. T. Lim, S. C. J. Loo and X. Chen, *Acc. Chem. Res.*, 2013, **46**, 782–791.
35 C. Y. Tay, P. Cai, M. I. Setyawati, W. Fang, L. P. Tan, C. H. L. Hong, X. Chen and D. T. Leong, *Nano Lett.*, 2014, **14**, 83–88.
36 K. Krumova, L. E. Greene and G. Cosa, *J. Am. Chem. Soc.*, 2013, **135**, 17135–17143.
37 L. Wang, Y. Xiao, W. Tian and L. Deng, *J. Am. Chem. Soc.*, 2013, **135**, 2903–2906.